Identify Anticancer Effects of Toona Sinensis Leaves through MEK/ERK signaling pathway in Human Glioblastoma Cells

Cheng Yu Tsai
Kaohsiung Medical University Hospital
Tai-Hsin Tsai
Kaohsiung Medical University Hospital
Huey-Jiun Ko
Kaohsiung Medical University
Keng-Liang Kuo
Kaohsiung Medical University Hospital
Chieh-Hsin Wu
Kaohsiung Medical University Hospital
Hui-Yuan Su
Kaohsiung Medical University Hospital
Ann-Shung Lieu
Kaohsiung Medical University Hospital
Aij-Lie Kwan
Kaohsiung Medical University Hospital
Joon-Khim Loh
Kaohsiung Medical University Hospital
Chih-Lung Lin
Kaohsiung Medical University Hospital
Yi-Ren Hong
Kaohsiung Medical University
Yu-Feng Su (suyufeng2000@yahoo.com.tw)
Kaohsiung Medical University Hospital

Research Article

Keywords: toona sinensis, glioblastoma multiforme, reactive oxygen species, MEK/ERK, GBM

Posted Date: July 28th, 2022

DOI: https://doi.org/10.21203/rs.3.rs-1837153/v1

Abstract

Introduction:

Toona sinensis is a traditional Chinese medicine commonly used in South-East Asia. The aqueous extracts of T. sinensis leaves (TSL) exhibit anticancer effects in various types of cancer. In this study, we assessed the effectiveness of TSL treatment for glioblastoma multiforme (GBM).

Methods

After treating A172 and U251 GBM with TSL, cell cycle and apoptotic cells were evaluated by flow cytometry, as well as anti-proliferative efficacy by MTT assay. Reactive oxygen species (ROS) and ATP production were quantified by CellROX, Dihydroethidium (DHE) and Tetramethylrhodamine methyl ester (TMRM). Apoptosis and MEK/ERK pathway related protein levels were detected by western blot.

Results

TSL treatment induced cell cycle arrest at G2/M and apoptosis. It also caused excessive ROS and decreased ATP production via blockage of electron transport chain (ETC) complexes, leading to ROS regulated mitochondrial dysfunction. Under TSL treatment in two GBM cells, the Bax and Puma protein level were elevated whereas Bcl-2 was descended. The mitochondria-mediated apoptosis and caspase-dependent pathway related proteins including cleaved caspase-3, cleaved caspase-9, and cleaved PARP were induced. Finally, U0126 as an inhibitor of MEK/ERK kinase was applied to demonstrate that the MEK/ERK pathway was responsible for the inhibition of ROS-regulated mitochondrial dysfunction and promoted apoptosis.

Conclusion

TSL treatment suppressed MEK/ERK activation to induce apoptosis through ROS-regulated mitochondrial dysfunction in GBM cells and provide a therapeutic potential in GBM therapy.

Background

Glioblastoma multiforme (GBM) is one of the most devastating tumors, with poor prognosis and high recurrence rates. It was recognized as grade IV astrocytoma according to the World Health Organization [1] and accounts for 40% of all primary brain tumors and 78% of malignant central nervous system tumors [2]. Even after standard surgical excision and concomitant radiation and chemotherapy (CCRT), the mean survival time remains < 15 months [3, 4]. The poor prognosis of GBM is related to glioma cells' natural invasive characteristics and therapeutic resistance, including chemoresistance and radioresistance [5]. The current standard chemotherapy for GBM is temozolomide, an oral alkylating

agent that induces G2/M arrest, leading to apoptosis [6, 7]. However, the overexpression of O6-53 methylguanine methyltransferase (MGMT) in GBM cells can reverse the methylation of the O6 position of guanine, causing DNA damage repair and chemoresistance [8, 9]. Therefore, developing new strategy agents for GBM is paramount.

Chemotherapy and radiation therapy share common pathways to cell death, inducing direct or indirect DNA damage through the generation of ROS [10]. Although low levels of mitochondrial ROS enhance cell growth, higher levels induce apoptosis [11, 12]. Thus, in many cancers, the ROS production level is an important marker of the state of the tumor and increasing ROS generation is considered an anticancer effect. High ROS levels induce cytotoxicity and reverse chemotherapeutic resistance in tumorigenic cells, and ROS production causes therapy resistance [13, 14]. In essence, ROS production is induced by mitochondrial dysfunction or mitochondrial dysfunction from redox aberrations (e.g., hypoxia, cellular degradation, or detoxification processes) and may synergistically promote cancer progression, even in the presence of drug resistance [15]. Thus, regulation of ROS-regulated mitochondrial dysfunction is a promising anticancer factor.

Toona sinensis (A. Juss) M.J. Roem., is a type of edible vegetable that is widely applied in South-East Asia as a type of traditional Chinese medicine (TCM) in clinical practice [16]. The most abundant ingredients in *T. sinensis* leaf (TSL) extracts include gallic acid (10%), rutin (0.5%), quercetin (0.42%), quercitrin (0.15%), kaempferol 3-O-b-D-glucoside (0.06%), methyl gallate (0.02%), ethyl gallate (0.002%), quercetin 3-O-b-D-glucoside (< 0.002%), and kaempferol (< 0.002%) [17]. TSL aqueous extracts have various biopharmacological activities, including antioxidant[18, 19], antidiabetes [20], neuron degenerative disease–suppressing [21], anti-inflammation [22], antivirus [23], and anticancer [24, 25] properties. TSL treatment inhibits cancer cell growth in lung cancer [26], prostate cancer [25], and acute myeloid leukemia [27]. JAK2/stat3, Akt, MEK/ERK, and mTOR/HIF-2α pathways have also been reported as potential pathways for inhibition of renal carcinoma cell growth and migration under TSL treatment [28]. However, the underlying molecular mechanisms remain unclear.

In this study, we explored if and how TSL treatment affects GBM. We demonstrated that TSL treatment induced apoptosis and cell cycle arrest to exert cytotoxic effects in two glioblastoma cell lines. ROS-regulated mitochondrial dysfunction was detected and the exhibition of ROS increased, followed by a decrease in mitochondrial transmembrane potential (ΔΨm) and ATP production under TSL treatment. Intrinsic mitochondria-mediated apoptosis and the caspase-dependent pathway were also detected by an increase in BAX/Puma and decrease in Bcl-2, accompanied by increased cleaved caspase-3, cleaved caspase-9, and cleaved caspase-PARP. The MAPK/ERK signaling pathway was responsible for the potential pathway through the use of U0126. Finally, our findings revealed that TSL treatment can induce apoptosis through ROS-regulated mitochondrial dysfunction through the MEK/ERK signaling pathway in human glioblastoma cells.

Materials And Methods

Materials

TMRM Reagent, CellROX™ Green Reagent were purchased from Invitrogen (Life Technologies, CA, USA). Bovine serum albumin (BSA), RNase A, propidium iodide (PI), carbobenzoxy-valyl-alanyl-aspartyl-[O-methyl]- fluoromethylketone (Z-VAD-FMK), Dihydroethidium (DHE), ATP Assay Kit were purchased from Sigma-Aldrich (St. Louis, MO, USA). MEK Inhibitor U0126 was purchased from Promega (Madison, WI, USA). Cell counting Kit-8 (CCK-8) was purchased from Targetmol (Shanghai, China). Annexin V-FITC/PI apoptosis detection kit was purchased from Fremont (CA, USA). The antibody specific for GAPDH was purchased from Santa Cruz Biotechnology (Santa Cruz, CA, USA). The antibodies specific for phospho-ERK1/2 (T202/Y204), ERK1/2, puma, Bax, Bcl-xL, Caspase-3, Caspase-9 and PARP were purchased from were purchased from Cell Signaling Technology (Beverly, MA, USA). The antibodies specific for total OXPHOS rodent WB antibody cocktail (Mouse) was purchased from Abcam (Cambridge, MA, USA). Secondary horseradish peroxidase (HRP) conjugated donkey anti-rabbit and donkey anti-mouse were obtained from Invitrogen (Life Technologies, CA, USA).

Preparation of Aqueous Extracts of Toona Sinensis Leaf (TSL)

The TS leaves used in this preparation were obtained from TS grown in Tuku (Yunlin County, Taiwan) and were picked and washed thoroughly with water. A voucher specimen (FY-001) was characterized by Dr. Horng-Liang Lay, Graduate Institute of Biotechnology, National Pingtung University of Science and Technology, Pingtung County, Taiwan, and deposited at Fooyin University, Kaohsiung. Permissions were also obtained by Dr. Horng-Liang Lay. In brief, the liquid of TSL was concentrated in a vacuum and freeze-dried to form a powder. The TSL aqueous extracts used in experiments were dissolved in sterile phosphate-buffered saline (PBS; pH 7.4) and filtered using a 0.45-mm syringe filter (Satorius Stedim Biotech Inc., Goettingen, Germany) [29].

Cell culture

Human GBM cell lines (A172 [ATCC CRL-1620; ATCC] and U251 [ormerly known as U-373 MG; ECACC 09063001]) were obtained from American Type Culture Collection, (ATCC, Manassas, VA, USA). The culture of A172 and U251 cells was performed in Dulbecco's Modified Eagle Medium (DMEM) containing 10% fetal bovine serum (FBS) and 1% penicillin–streptomycin (100 units/ml of penicillin and 10 mg/ml of streptomycin; all from Gibco; Thermo Fisher Scientific, Waltham, MA, USA) and incubated in a 5% CO2 incubator at 37 °C with fully humidified conditions. All experiments were performed when cells were in the logarithmic phase of growth.

Cell viability and colony formation assay

An CCK-8 assay was used to measure cell viability. Briefly, GBM cells, A172 (4×103 cells/well) and U251 (4×103 cells/well), were seeded in 96-well plates overnight, and were then incubated with various concentrations of TSL at 37°C for 24, 48 and 72 h. After that, add 1/10 volume of Cell Counting Kit-8 (CCK-8) directly to cells in culture medium. Incubate in a cell culture incubator for 1 to 4 hours at 37°C

until the color turns orange. Using a Synergy™ HT Multi-Detection Reader (Bio-Tek Instruments, Winooski, VT) absorbance was measured at 450 nm. In addition, colony formation assays were conducted as described previously [30]. Cells were then rinsed with distilled water, air-dried, and colonies were counted and analyzed using ImageJ software. Then, DMSO was added to dissolve this crystal. The results are expressed as the average colony count ± SE from three independent experiments.

Cell cycle analysis

For cell cycle analysis, cultured A172 and U251 cells, following treatment with increasing concentrations of TSL for 48 h, were collected and washed with PBS (pH 7.2). The cells were resuspended in 85% methanol for overnight at 4 °C and then centrifuged at 1500rpm for 10 min. The resultant pellet was washed twice with PBS, suspended in PBS and incubated with stained with 100 µg/mL propidium iodide (PI, Sigma-Aldrich Co) and RNase (20 Units/mL, final concentration) for 30 min. At least 10,000 cells were counted by a flow cytometer (Attune NxT flow cytometer, Thermo Fisher Scientific), and the data obtained were analyzed using and the data obtained were analyzed using Attune NxT Flow Cytometer Software (Thermo Fisher Scientific).

Apoptosis analysis

Apoptosis of A172 and U251 cells treated with various concentrations of TSL in the presence or absence of z-VAD (10 µM) or U0126 (10 µM) for 48 h was determined by the CF®488A Annexin V and PI Apoptosis kit. Phosphatidylserines exposed on the membrane surface of apoptotic cells were stained with Annexin V-FITC according to the manufacturer's instructions. The late apoptotic (or necrotic) cells were stained with PI. Parallel sets of wells containing non-treated A172 or U251 were regarded as the (+) controls. The results were acquired and analyzed with Attune NxT Flow Cytometer Software (Thermo Fisher Scientific). The population of apoptotic cells was characterized by its high mean fluorescence of Annexin V-FITC in a flow cytometric histogram.

Determination of the intracellular ROS, mitochondrial ROS and Mitochondrial Membrane Potential (ΔΨm)

Intracellular ROS production was detected using CellROX, mitochondrial ROS production was detected using Dihydroethidium (DHE) and ΔΨm production was detected using Tetramethylrhodamine methyl ester (TMRM). Following incubation A172 and U251 cells with the different doses of TSL for 48 h, 5 µM CellROX® green reagent, 250 nM DHE red reagent and 25 nM TMRM at 37 °C for 30 min. Subsequently, the cells were washed in PBS, trypsinized and measured fluorescence intensity by flow cytometry at excitation/emission wavelengths of 485/530 nm, 510/580 nm and 488/570 nm for CellROX, DHE and TMRM, respectively, and the results were analyzed using Attune NxT Flow Cytometer Software.

Cell ATP levels

Cultured A172 and U251 cells, following treatment with increasing concentrations of TSL for 48 h, were collected and washed with PBS (pH 7.2). Cell ATP measurement were conducted as described previously [31]. Then sample was measured with absorbance at 570 nm (A570) or the fluorescence (FLU, lex = 535/

lem = 587 nm) in a microplate reader. For each measurement, a standard curve will be constructed using serial dilutions of ATP stock solution. The sample was converted to nanomolar amounts of ATP accordingly. The results are expressed as the average colony count ± SE from three independent experiments.

Western blot analysis

Cells were seeded into 10 cm dish plates, treated different concentrations of TSL in the presence or absence of z-VAD (10 μM) or U0126 (10 μM) for 48 h. Cell lysis, protein concentration, SDS-PAGE gel and western blotting were performed as described previously [32]. The following antibodies dilutions were used for immunodetection: PARP (1:1,000, Cell signaling, Beverly, MA, USA); caspase-3 (1:1,000, Cell signaling, Beverly, MA, USA); caspase-9 (1:1,000, Cell signaling, Beverly, MA, USA); Bcl-2 (1:1,000, Cell signaling, Beverly, MA, USA); Bax (1:1,000, Cell signaling, Beverly, MA, USA); puma (1:1,000, Cell signaling, Beverly, MA, USA); ERK1/2 (1:1,000, Cell signaling, Beverly, MA, USA); phospho-ERK1/2 (T202/Y204,1:1,000, Cell signaling, Beverly, MA, USA); GAPDH (1:5,000, Santa Cruz biotechnology, Heidelberg, Germany).

Statistical Analysis

Data are presented as mean ± standard deviation. Statistical analyses were performed using one-way analysis of variance. Data were compared using Student's t-test. The level of statistical significance was set at * $p < 0.05$, ** $p < 0.01$, *** $p < 0.001$.

Statement

All methods were carried out in accordance with relevant guidelines and regulations.

Results

TSL treatment induced cytotoxic effects that decreased the growth and proliferation of GBM cells

To examine the cytotoxic effect of *T. sinensis* in glioblastoma cells, we treated the two glioblastoma cell lines (A172 and U251) with TSL aqueous extract. To assess cell proliferation and cell viability, an MTT assay was performed with TSL under different concentrations (10, 20, 40, 80, and 160 μg/mL) at 24, 48, and 72 h. The results revealed that the cytotoxic effect of TSL increased in both a dose-dependent and time-dependent manner (Figure 1A). Colony formation assay also revealed that TSL dose-dependently suppresses the glioblastoma cells (Figure 1B). We also investigated the morphologic characteristics of two glioblastoma cells that were treated with TSL under various concentrations (10, 20, 40, 80, and 160 μg/mL) for 48 h. Phase-contrast micrographs revealed that the aqueous extract of TSL dose-dependently induced cell shrinkage and apoptotic vacuoles, presenting as clusters of dying cells (CDC) in both the glioblastoma cell lines (Figure 1C). Therefore, these data revealed that aqueous extracts of TSL treatment decreased the growth and proliferation of and exerted a cytotoxic effect on GBM cells.

TSL treatment induced cell cycle arrest and apoptosis in GBM cells

Cell cycle arrest and apoptosis are the major cytotoxic effects of cancer treatment. We investigated whether TSL treatment (10, 20, 40, and 80 μg/mL) induced cell cycle arrest and apoptosis in the A172 and U251 cell lines. The results revealed that TSL treatment dose-dependently induced G2/M arrest in both the cell lines (29.87% in A172 and 31.27% in U251) (Figure 2A). Moreover, flow cytometry revealed that TSL treatment yielded a high percentage of apoptosis cells in the A172 and U251 cell lines (Figure 2B). Through detailed characterization of the effect of TSL treatment on cell cycle progression, we observed that TSL treatment induced a time-dependent accumulation of G2/M phase cells in the GBM cell lines. The results revealed that TSL treatment can induce cell cycle arrest, thereby suppressing cell proliferation and promoting apoptosis in GBM cells.

TSL treatment caused ROS-related mitochondrial dysfunction in GBM cells

Mitochondrial dysfunction is essential for cellular energy metabolism and cell apoptosis. Excessive ROS and decreased mitochondrial oxidative phosphorylation complexes (OX-PHOS complexes) caused a reduction in the ΔΨm and ATP production, which led to mitochondrial dysfunction. To further examine whether TSL treatment induced ROS production in glioblastoma cells, we used Western blotting analysis to examine mitochondrial OXPHOS complexes, because they directly affect mitochondrial function. The results revealed significantly reduced levels of complex I, II, and IV proteins (Figure 3A). The normalized ATP measurements, mitochondrial ROS, cytosolic ROS, and ΔΨm levels were measured using flow cytometry and fluorescence microscopy with DHE deep red, CellROX deep green, and TMRM deep red staining and presented as the mean fluorescent intensity (MFI) or percentage of the cells. The results revealed that ATP levels were significantly decreased under TSL treatment in a dose-dependent manner in the A172 and U251 cell lines (Figure 3B). In addition, mitochondrial and cytosolic ROS levels were increased under TSL treatment in a dose-dependent manner (Figure 3C, D). Eventually, ΔΨm levels were attenuated under TSL treatment in both the cell lines (Figure 3E). Collectively, the results confirmed that TSL treatment dose-dependently induced ROS-related mitochondrial dysfunction, which is affected by mitochondrial complexes I, II, and IV, in GBM cells.

TSL treatment induced apoptosis by intrinsic mitochondria-mediated apoptosis and caspase-dependent pathways in GBM cells

Multiple death signals influence mitochondrial dysfunction during apoptosis. The expression of proapoptotic factors, such as BCL-2-associated X protein (Bax), Puma, and antiapoptotic factor (Bcl-2), play a critical role in intrinsic mitochondria-mediated apoptosis. Moreover, apoptosis is an organized energy-dependent process of cellular self-destruction conducted by proteolytic enzymes, such as the caspase-dependent pathway. Therefore, we first investigated the involvement of proapoptotic proteins (Bax and Puma) and antiapoptotic protein (Bcl-2). The results revealed that TSL treatment increased proapoptotic Bax/Puma protein levels and decreased antiapoptotic Bcl2 protein levels in both the glioblastoma cells (Figure 4A). Furthermore, TSL treatment increased the protein levels of cleaved caspase-3, cleaved caspase-9, and cleaved PARP (Figure 4B). To verify apoptosis through the caspase-

dependent pathway, we used z-VAD-FMK to treat the glioblastoma cells after TSL treatment. Flow cytometry and Western blotting results revealed a decreased percentage of apoptosis cells and protein levels of cleaved caspase-3, cleaved caspase-9, and cleaved PARP (Figure 4C, D). Taken together, we demonstrated that TSL treatment induced apoptosis through intrinsic mitochondria-mediated apoptosis and caspase-dependent pathways in GBM cells.

TSL treatment induced apoptosis through ROS-regulated mitochondrial dysfunction by inhibiting MEK/ERK signaling pathway in GBM cells

Accumulating evidence indicates that the antiapoptotic function of the MEK/ERK pathway inhibits mitochondrial dysfunction. Therefore, we speculated whether TSL treatment induced apoptosis through mitochondrial dysfunction by inhibiting the *mitogen-activated protein kinase/ extracellular signal-regulated kinase* (MAPK/ERK) signaling pathway. First, we examined the expression level of ERK/p-ERK under TSL treatment in glioblastoma cells. The results revealed a low expression level of p-ERK under TSL treatment in glioblastoma cells in a dose-dependent manner (Figure 5A). We then used U0126, a highly selective inhibitor of both MEK1, and MEK2, a type of MAPK/ERK kinase. The flow cytometry data indicated that the increase in apoptosis cells was greater in the TSL and U0126 groups in both glioblastoma cells (Figure 5B). Moreover, the caspase-dependent system (cleaved caspase-3, cleaved caspase-9, and cleaved PARP) and proapoptotic protein (Bax) were increased, and the decreases in the levels of ERK/p-ERK and anti-apoptotic protein (Bcl-2) were greater in the TSL and U0126 groups (Figure 5C, D). Due to above findings, we found ERK activation is required for apoptosis induction by TSL treatment in GBM cells

Effect of MAPK inhibitors on mitochondrial function subjected to TSL in GBM cells

Finally, we used MAPK inhibitors to elucidate whether it is responsible in mitochondria function to induce apoptosis under TSL treatment. The normalized ATP measurements, mitochondrial ROS, cytosolic ROS, and ΔΨm levels were measured under TSL and MAPK inhibitors (U0126). The results revealed that, and ATP production were attenuated under TSL and U0126 group (Fig.6A). Oppositely, mitochondrial ROS, cytosolic ROS were enhanced, and ΔΨm levels were decreased under TSL and U0126 group (Fig. 6B, C, D). Finally, we elucidated the inhibition of MAPK/ERK signaling pathway could be the potential pathway to induce apoptosis by ROS-regulated mitochondria dysfunction in GBM cells under TSL treatment.

Discussion

In this study, we evidenced that TSL treatment induced cytotoxic effects to offer antitumor effects in two GBM cell lines. TSL treatment induced cell cycle arrest at G2/M and apoptosis through mitochondrial dysfunction through ETC complex inhibition and ROS overproduction. We further clarified that the MEK/ERK signaling pathway is responsible for the underlying molecular mechanisms. This is the first study to demonstrate that TSL can induce apoptosis to exert a cytotoxic effect through the inhibition of the MEK/ERK signaling pathway and can be a new therapy for GBM treatment.

For traditional GBM chemotherapy, temozolomide is the most widely used and essential agent, which, through the formation of O6-methylguanine, mismatches with thymine in subsequent DNA replication cycles to induce cell cycle arrest in G2/M and then exerts a cytotoxic effect. This has been demonstrated to lead to several cellular outcomes, such as apoptosis [33] and autophagy [34] in GBMs. However, the ability of resistance to temozolomide was modulated by MGMT, which is considered therapy resistance and recurrence in clinical practice. Therefore, the development of new strategies for GBM treatment is an urgent need. According to evidence of the early apoptotic process and that the central coordinator of cell death is particularly affected by mitochondria, mitochondrial function is a crucial factor influencing apoptosis [35]. Mitochondrial dysfunction is caused by the production of excessive ROS, which induces oxidative stress and damages the mitochondrial ETC complexes. Excessive ROS also damage ETC complexes through blockade of electron transfer, which leads to electron leaking. In particular, ETC complex IV blockade was more likely to cause reduced ATP synthesis [36]. In our study, TSL treatment also induced cell cycle arrest in G2/M and led to apoptosis consistent with the temozolomide-mediated effect. Our results also indicated that mitochondrial ROS and cytosolic ROS were increased, and ΔΨm levels were decreased as a late event in the apoptotic process. Furthermore, our data indicated that complexes I, II, and IV were predominately decreased. Collectively, TSL treatment induced ROS-regulated mitochondrial dysfunction and promoted apoptosis, thus exerting a cytotoxic effect in GBM cell lines.

Proapoptotic protein Bax and antiapoptotic protein Bcl-2 are necessary for mitochondrial outer membrane permeabilization and transduction of the cell death signal by the mitochondria [37]. Bcl-2 protein plays a regulatory role in the mitochondrial-related intrinsic apoptotic pathway and exerts limited resistance to standard cancer treatments. A balance of Bax and Bcl-2 proteins is essential for apoptosis. Upregulation of Bax and downregulation of Bcl-2 were as many anticancer effects as possible. Moreover, Puma binds to the antiapoptotic BCL-2 members and inhibits their prosurvival activity, and it can also directly activate the proapoptotic effector BAX to damage mitochondrial outer membrane permeabilization, resulting in the release of apoptogenic molecules [38]. Our data revealed that TSL treatment induced the levels of proapoptotic Bax and Puma and decreased the antiapoptotic Bcl-2 expression level through the mitochondrial-related intrinsic pathway. Moreover, our results revealed that TSL induced the activation of cleaved caspase-3, cleaved caspase-9, and cleaved PARP, which preceded the onset of caspase-dependent apoptosis. Taken together, we demonstrated that TSL treatment induced apoptosis through intrinsic mitochondrial-mediated apoptosis and caspase-dependent pathways in GBM cell lines.

Regarding the underlying molecular mechanisms, the MEK/ERK signaling pathway plays a vital role in the control of key cellular processes, including cell survival and proliferation. MEK/ERK dysregulation promotes cancer cell growth, and ERK activation plays a key role in cancer malignancy [39]. ERK1/2 activation generally promotes cell proliferation and leads to cancer formation [40]. Our results revealed that TSL treatment suppresses ERK and p-ERK and induced ROS-regulated mitochondrial dysfunction and apoptosis. Next, U0126 was used as an inhibitor of MAPK/ERK kinase. The results demonstrated that p-ERK was more suppressed, and apoptosis was obviously induced. The expression of intrinsic mitochondrial-mediated apoptotic proteins (Bax/Puma) and caspase-dependent proteins (cleaved

caspase-3, cleaved caspase-9, and cleaved PARP) was also clearly increased. In addition, mitochondrial ROS and cytosolic ROS were considerably increased, and the levels of ΔΨm and ATP production were obviously decreased in the TSL and U0126 groups. Finally, our results demonstrated that TSL treatment induced apoptosis through ROS-regulated mitochondrial dysfunction via the MEK/ERK pathway.

In this study, we proposed a model summarizing the results as in Fig. 7. TSL treatment inhibited MEK/ERK activation, which induced increased mitochondrial ROS production and decreased ATP production, thereby inducing mitochondrial dysfunction. Moreover, upregulation of proapoptotic proteins (Bax and Puma) and downregulation of antiproapoptotic protein (Bcl-2) were also demonstrated. Finally, caspase-dependent apoptosis was induced as a last event under TSL treatment in GBM cell lines.

Conclusions

In Summary our study revealed that the TSL aqueous extract exhibited antitumor activities in A172 and U251 GBM cells. First, TSL induced cytotoxic effects via cell cycle arrests at G2/M phase and apoptosis. Second, TSL treatment caused mitochondrial dysfunction with an increase in mitochondrial ROS production and impairment of complexes I, II, and IV. TSL also promoted intrinsic mitochondria-mediated apoptosis and caspase-dependent pathways in GBM cells. Third, MEK/ERK signaling pathways can be inactivated following TSL treatment as a potential molecular pathway and could be a potential therapy for GBM treatment. Future research should investigate the effective, unknown components of the MEK/ERK signaling pathway for GBM therapy in an in vivo xenograft model.

Abbreviations

TSL
Toona Sinensis Leaves
ROS
Reactive oxygen species
DHE
Dihydroethidium
TMRM
Tetramethylrhodamine methyl ester
ETC
Electron transport chain
CCRT
Concomitant radiation and chemotherapy
MGMT
Methylguanine methyltransferase
ΔΨm
Mitochondrial transmembrane potential
BSA

Bovine serum albumin

PI

Propidium iodide

Z-VAD-FMK

Carbobenzoxy-valyl-alanyl-aspartyl-[O-methyl]- fluoromethylketone

CCK-8

Cell counting Kit-8

FBS

Fetal bovine serum

DMEM

Dulbecco's Modified Eagle Medium

PVDF

Polyvinylidene difluoride

CDC

Clusters of dying cells

OX-PHOS

Mitochondrial oxidative phosphorylation

MFI

Mean fluorescent intensity

Bax

BCL-2-associated X

MAPK/ERK

Mitogen-activated protein kinase/ extracellular signal-regulated kinase

Declarations

Ethics approval and consent to participate

Not applicable.

Consent for publication

Not applicable.

Availability of data and materials

All data generated or analysed during this study are included in this published article.

Competing interests

The authors declare that they have no competing interests.

Funding

The present research was supported by grants KMUH110-0M27 from Kaohsiung Medical University Hospital, KMTTH-107-028, KMTTH-108-011 and KMTTH-109-037 from Kaohsiung Municipal Ta-Tung Hospital. We thank Wallace Academic Editing for English edition on the manuscript.

Authors' contributions

CYT, THT, HJK, YFS design of the work. All other experiments were performed by CYT, HJK. CYT, HJK analysis. THT, KLK, CHW, HYS, ASL, ALK, JKL, CLL, YRH interpretation of data. All authors contributed to manuscript revision and approved the final version. All authors have read and agreed to the published version of the manuscript.

Acknowledgements

Not applicable.

Authors' information (optional)

Division of Neurosurgery, Department of Surgery, Kaohsiung Medical University Hospital, Kaohsiung 80756, Taiwan.

Cheng Yu Tsai, Tai-Hsin Tsai, Keng-Liang Kuo, Chieh-Hsin Wu, Hui-Yuan Su, Ann-Shung Lieu, Aij-Lie Kwan, Joon-Khim Loh, Chih-Lung Lin and Yu-Feng Su.

Department of Surgery, Post Baccalaureate Medicine, College of Medicine, Kaohsiung Medical University, Kaohsiung 80756, Taiwan.

Cheng Yu Tsai, and Yu-Feng Su.

Department of Surgery, School of Medicine, College of Medicine, Kaohsiung Medical University, Kaohsiung 80756, Taiwan.

Cheng Yu Tsai, Tai-Hsin Tsai, Chieh-Hsin Wu, Ann-Shung Lieu, Aij-Lie Kwan, Joon-Khim Loh, Chih-Lung Lin and Yu-Feng Su.

Department of Biochemistry, College of Medicine, Kaohsiung Medical University, Kaohsiung, Taiwan.

Yi-Ren Hong.

Graduate Institute of Medicine, College of Medicine, Kaohsiung Medical University, Kaohsiung, Taiwan.

Yi-Ren Hong.

Department of Biological Sciences, National Sun Yat-Sen University, Kaohsiung, Taiwan.

Yi-Ren Hong.

References

1. Louis DN, Perry A, Reifenberger G, von Deimling A, Figarella-Branger D, Cavenee WK, Ohgaki H, Wiestler OD, Kleihues P, Ellison DW: **The 2016 World Health Organization Classification of Tumors of the Central Nervous System: a summary**. *Acta Neuropathol* 2016, **131**(6):803-820.
2. Miller CR, Perry A: **Glioblastoma**. *Arch Pathol Lab Med* 2007, **131**(3):397-406.
3. Park JK, Hodges T, Arko L, Shen M, Dello Iacono D, McNabb A, Olsen Bailey N, Kreisl TN, Iwamoto FM, Sul J *et al*: **Scale to predict survival after surgery for recurrent glioblastoma multiforme**. *J Clin Oncol* 2010, **28**(24):3838-3843.
4. Stupp R, Mason WP, van den Bent MJ, Weller M, Fisher B, Taphoorn MJ, Belanger K, Brandes AA, Marosi C, Bogdahn U *et al*: **Radiotherapy plus concomitant and adjuvant temozolomide for glioblastoma**. *N Engl J Med* 2005, **352**(10):987-996.
5. Minniti G, Amelio D, Amichetti M, Salvati M, Muni R, Bozzao A, Lanzetta G, Scarpino S, Arcella A, Enrici RM: **Patterns of failure and comparison of different target volume delineations in patients with glioblastoma treated with conformal radiotherapy plus concomitant and adjuvant temozolomide**. *Radiother Oncol* 2010, **97**(3):377-381.
6. Lee SY: **Temozolomide resistance in glioblastoma multiforme**. *Genes & Diseases* 2016, **3**(3):198-210.
7. Alonso MM, Gomez-Manzano C, Bekele BN, Yung WK, Fueyo J: **Adenovirus-based strategies overcome temozolomide resistance by silencing the O6-methylguanine-DNA methyltransferase promoter**. *Cancer Res* 2007, **67**(24):11499-11504.
8. Le Rhun E, Preusser M, Roth P, Reardon DA, van den Bent M, Wen P, Reifenberger G, Weller M: **Molecular targeted therapy of glioblastoma**. *Cancer Treat Rev* 2019, **80**:101896.
9. Cabrini G, Fabbri E, Lo Nigro C, Dechecchi MC, Gambari R: **Regulation of expression of O6-methylguanine-DNA methyltransferase and the treatment of glioblastoma (Review)**. *Int J Oncol* 2015, **47**(2):417-428.
10. Trachootham D, Zhou Y, Zhang H, Demizu Y, Chen Z, Pelicano H, Chiao PJ, Achanta G, Arlinghaus RB, Liu J *et al*: **Selective killing of oncogenically transformed cells through a ROS-mediated mechanism by beta-phenylethyl isothiocyanate**. *Cancer Cell* 2006, **10**(3):241-252.
11. Circu ML, Aw TY: **Reactive oxygen species, cellular redox systems, and apoptosis**. *Free Radic Biol Med* 2010, **48**(6):749-762.
12. García-Ruiz C, Colell A, Marí M, Morales A, Fernández-Checa JC: **Direct Effect of Ceramide on the Mitochondrial Electron Transport Chain Leads to Generation of Reactive Oxygen Species: ROLE OF MITOCHONDRIAL GLUTATHIONE***. *Journal of Biological Chemistry* 1997, **272**(17):11369-11377.
13. Aggarwal V, Tuli HS, Varol A, Thakral F, Yerer MB, Sak K, Varol M, Jain A, Khan MA, Sethi G: **Role of Reactive Oxygen Species in Cancer Progression: Molecular Mechanisms and Recent Advancements**. *Biomolecules* 2019, **9**(11).
14. Lin Y-H: **MicroRNA Networks Modulate Oxidative Stress in Cancer**. *International journal of molecular sciences* 2019, **20**(18):4497.

15. Okon IS, Zou MH: **Mitochondrial ROS and cancer drug resistance: Implications for therapy**. *Pharmacol Res* 2015, **100**:170-174.
16. Edmonds JM, Staniforth M: **Plate 348. Toona sinensis**. *Curtis's Botanical Magazine* 1998, **15**(3):186-193.
17. Sun X, Zhang L, Cao Y, Gu Q, Yang H, Tam JP: **Quantitative Analysis and Comparison of Four Major Flavonol Glycosides in the Leaves of Toona sinensis (A. Juss.) Roemer (Chinese Toon) from Various Origins by High-Performance Liquid Chromatography-Diode Array Detector and Hierarchical Clustering Analysis**. *Pharmacogn Mag* 2016, **12**(Suppl 2):S270-276.
18. Yang HL, Chen SC, Lin KY, Wang MT, Chen YC, Huang HC, Cho HJ, Wang L, Kumar KJ, Hseu YC: **Antioxidant activities of aqueous leaf extracts of Toona sinensis on free radical-induced endothelial cell damage**. *J Ethnopharmacol* 2011, **137**(1):669-680.
19. Hseu YC, Chang WH, Chen CS, Liao JW, Huang CJ, Lu FJ, Chia YC, Hsu HK, Wu JJ, Yang HL: **Antioxidant activities of Toona Sinensis leaves extracts using different antioxidant models**. *Food Chem Toxicol* 2008, **46**(1):105-114.
20. Wang PH, Tsai MJ, Hsu CY, Wang CY, Hsu HK, Weng CF: **Toona sinensis Roem (Meliaceae) leaf extract alleviates hyperglycemia via altering adipose glucose transporter 4**. *Food Chem Toxicol* 2008, **46**(7):2554-2560.
21. Liao J-W, Hsu C-K, Wang M-F, Hsu W-M, Chan Y-C: **Beneficial effect of Toona sinensis Roemor on improving cognitive performance and brain degeneration in senescence-accelerated mice**. *British Journal of Nutrition* 2006, **96**(2):400-407.
22. Hsiang CY, Hseu YC, Chang YC, Kumar KJ, Ho TY, Yang HL: **Toona sinensis and its major bioactive compound gallic acid inhibit LPS-induced inflammation in nuclear factor-κB transgenic mice as evaluated by in vivo bioluminescence imaging**. *Food Chem* 2013, **136**(2):426-434.
23. Chen CJ, Michaelis M, Hsu HK, Tsai CC, Yang KD, Wu YC, Cinatl J, Jr., Doerr HW: **Toona sinensis Roem tender leaf extract inhibits SARS coronavirus replication**. *J Ethnopharmacol* 2008, **120**(1):108-111.
24. Chia YC, Rajbanshi R, Calhoun C, Chiu RH: **Anti-neoplastic effects of gallic acid, a major component of Toona sinensis leaf extract, on oral squamous carcinoma cells**. *Molecules* 2010, **15**(11):8377-8389.
25. Chen H-M, Wu Y-C, Chia Y-C, Chang F-R, Hsu H-K, Hsieh Y-C, Chen C-C, Yuan S-S: **Gallic acid, a major component of Toona sinensis leaf extracts, contains a ROS-mediated anti-cancer activity in human prostate cancer cells**. *Cancer Lett* 2009, **286**(2):161-171.
26. Wang CY, Lin KH, Yang CJ, Tsai JR, Hung JY, Wang PH, Hsu HK, Huang MS: **Toona sinensis extracts induced cell cycle arrest and apoptosis in the human lung large cell carcinoma**. *Kaohsiung J Med Sci* 2010, **26**(2):68-75.
27. Yang H-L, Kuo Y-T, Vudhya Gowrisankar Y, Lin K-Y, Hsu L-S, Huang P-J, Lin H-C, Hseu Y-C: **The Leaf Extracts of Toona sinensis and Fermented Culture Broths of Antrodia camphorata Synergistically**

Cause Apoptotic Cell Death in Promyelocytic Leukemia Cells. *Integrative Cancer Therapies* 2020, **19**:1534735420923734.

28. Chen Y-C, Chien L-H, Huang B-M, Chia Y-C, Chiu H-F: **Aqueous Extracts of Toona sinensis Leaves Inhibit Renal Carcinoma Cell Growth and Migration Through JAK2/stat3, Akt, MEK/ERK, and mTOR/HIF-2α Pathways**. *Nutrition and Cancer* 2016, **68**(4):654-666.
29. Su YF, Yang YC, Hsu HK, Hwang SL, Lee KS, Lieu AS, Chan TF, Lin CL: **Toona sinensis leaf extract has antinociceptive effect comparable with non-steroidal anti-inflammatory agents in mouse writhing test**. *BMC Complement Altern Med* 2015, **15**:70.
30. Tsai C-Y, Ko H-J, Chiou S-J, Lai Y-L, Hou C-C, Javaria T, Huang Z-Y, Cheng T-S, Hsu T-I, Chuang J-Y *et al*: **NBM-BMX, an HDAC8 Inhibitor, Overcomes Temozolomide Resistance in Glioblastoma Multiforme by Downregulating the β-Catenin/c-Myc/SOX2 Pathway and Upregulating p53-Mediated MGMT Inhibition**. *International journal of molecular sciences* 2021, **22**(11):5907.
31. Ko HJ, Tsai CY, Chiou SJ, Lai YL, Wang CH, Cheng JT, Chuang TH, Huang CF, Kwan AL, Loh JK *et al*: **The Phosphorylation Status of Drp1-Ser637 by PKA in Mitochondrial Fission Modulates Mitophagy via PINK1/Parkin to Exert Multipolar Spindles Assembly during Mitosis**. *Biomolecules* 2021, **11**(3).
32. Tsai CY, Ko HJ, Huang CF, Lin CY, Chiou SJ, Su YF, Lieu AS, Loh JK, Kwan AL, Chuang TH *et al*: **Ionizing Radiation Induces Resistant Glioblastoma Stem-Like Cells by Promoting Autophagy via the Wnt/β-Catenin Pathway**. *Life (Basel)* 2021, **11**(5).
33. Hermisson M, Klumpp A, Wick W, Wischhusen J, Nagel G, Roos W, Kaina B, Weller M: **O6-methylguanine DNA methyltransferase and p53 status predict temozolomide sensitivity in human malignant glioma cells**. *J Neurochem* 2006, **96**(3):766-776.
34. Kanzawa T, Germano IM, Komata T, Ito H, Kondo Y, Kondo S: **Role of autophagy in temozolomide-induced cytotoxicity for malignant glioma cells**. *Cell Death & Differentiation* 2004, **11**(4):448-457.
35. Henry-Mowatt J, Dive C, Martinou JC, James D: **Role of mitochondrial membrane permeabilization in apoptosis and cancer**. *Oncogene* 2004, **23**(16):2850-2860.
36. Chou CH, Loh JK, Yang MC, Lin CC, Hong MC, Cho CL, Chou AK, Wang CH, Lieu AS, Howng SL *et al*: **AIBp regulates mitotic entry and mitotic spindle assembly by controlling activation of both Aurora-A and Plk1**. *Cell Cycle* 2015, **14**(17):2764-2776.
37. Kale J, Osterlund EJ, Andrews DW: **BCL-2 family proteins: changing partners in the dance towards death**. *Cell Death & Differentiation* 2018, **25**(1):65-80.
38. Li M: **The role of P53 up-regulated modulator of apoptosis (PUMA) in ovarian development, cardiovascular and neurodegenerative diseases**. *Apoptosis* 2021, **26**(5):235-247.
39. Burotto M, Chiou VL, Lee JM, Kohn EC: **The MAPK pathway across different malignancies: a new perspective**. *Cancer* 2014, **120**(22):3446-3456.
40. Sugiura R, Satoh R, Takasaki T: **ERK: A Double-Edged Sword in Cancer. ERK-Dependent Apoptosis as a Potential Therapeutic Strategy for Cancer**. *Cells* 2021, **10**(10).

Figures

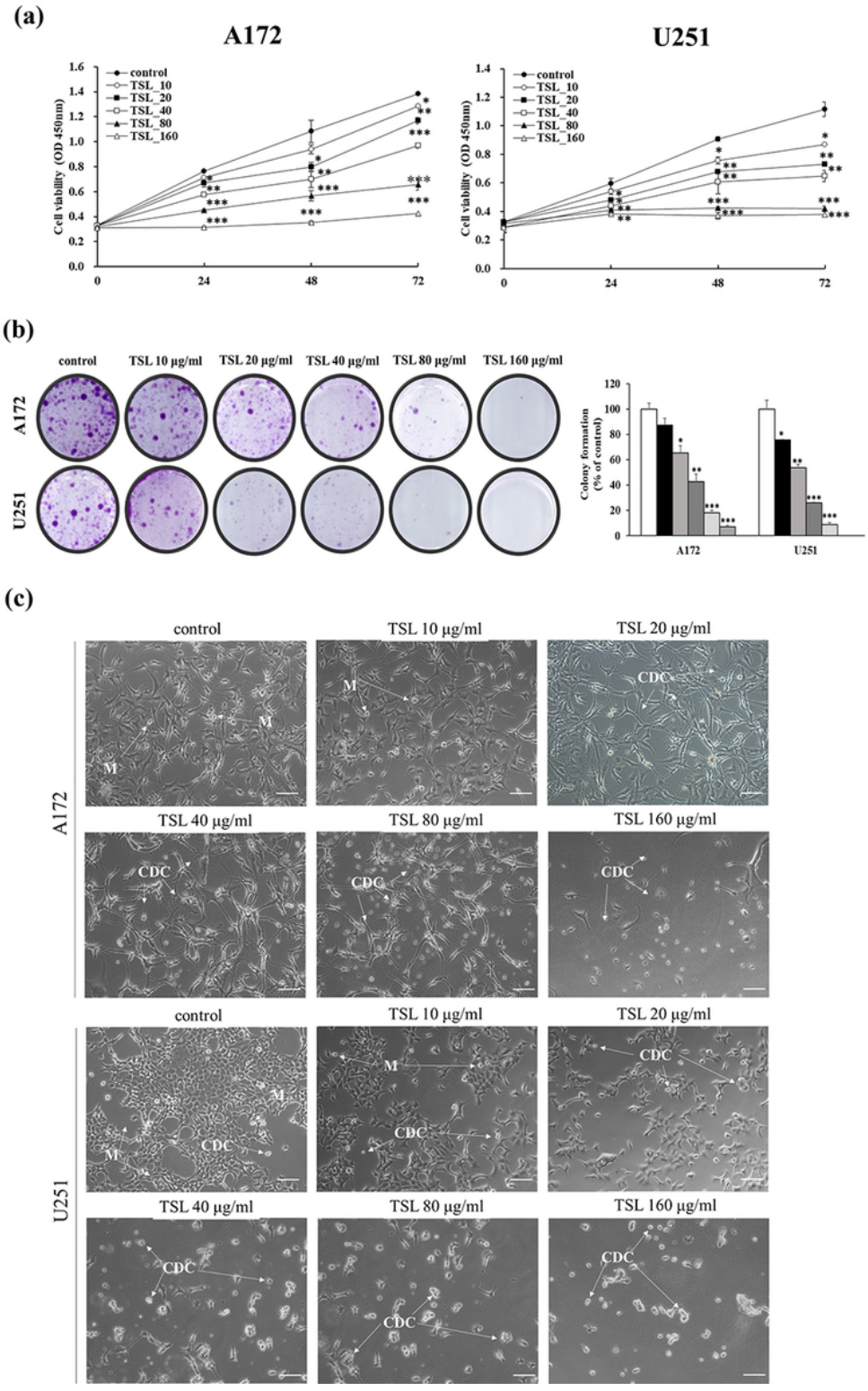

Figure 1

Effects of TSL on the viability and morphology of A172 and U251. (A) The cells (2 ×10^4 cells/well) were incubated with different concentrations of TSL for 24 to 72 h as described in Materials and Methods. Cell viability was measured by MTT test. (B) The long-term anti-proliferative effects were evaluated in a colony formation assay. A172 and U251 GBMs cell were incubated with different concentrations of (0, 10, 20, 40, 80 and 160 μg/ml) for 16 days and assayed for colony formation. The lower panel shows

quantitative analyses of colony formation. (C) Morphological illustrations of the anticancer effects observed after 48 h of culturing A172 and U251 GBMs cell with different concentrations of TSL by light microscopy (magnification ×100). The cells that are dying and detaching from the culture substrate appear white and refringent: they are labeled as clusters of dying cells (CDC). The round and refringent cells are undergoing mitosis (M). All results are shown as mean ± s.d. from three independent experiments; ***p<0.001, **P < 0.01, *P < 0.05 compared with the indicated control; scale bar = 100 μm.

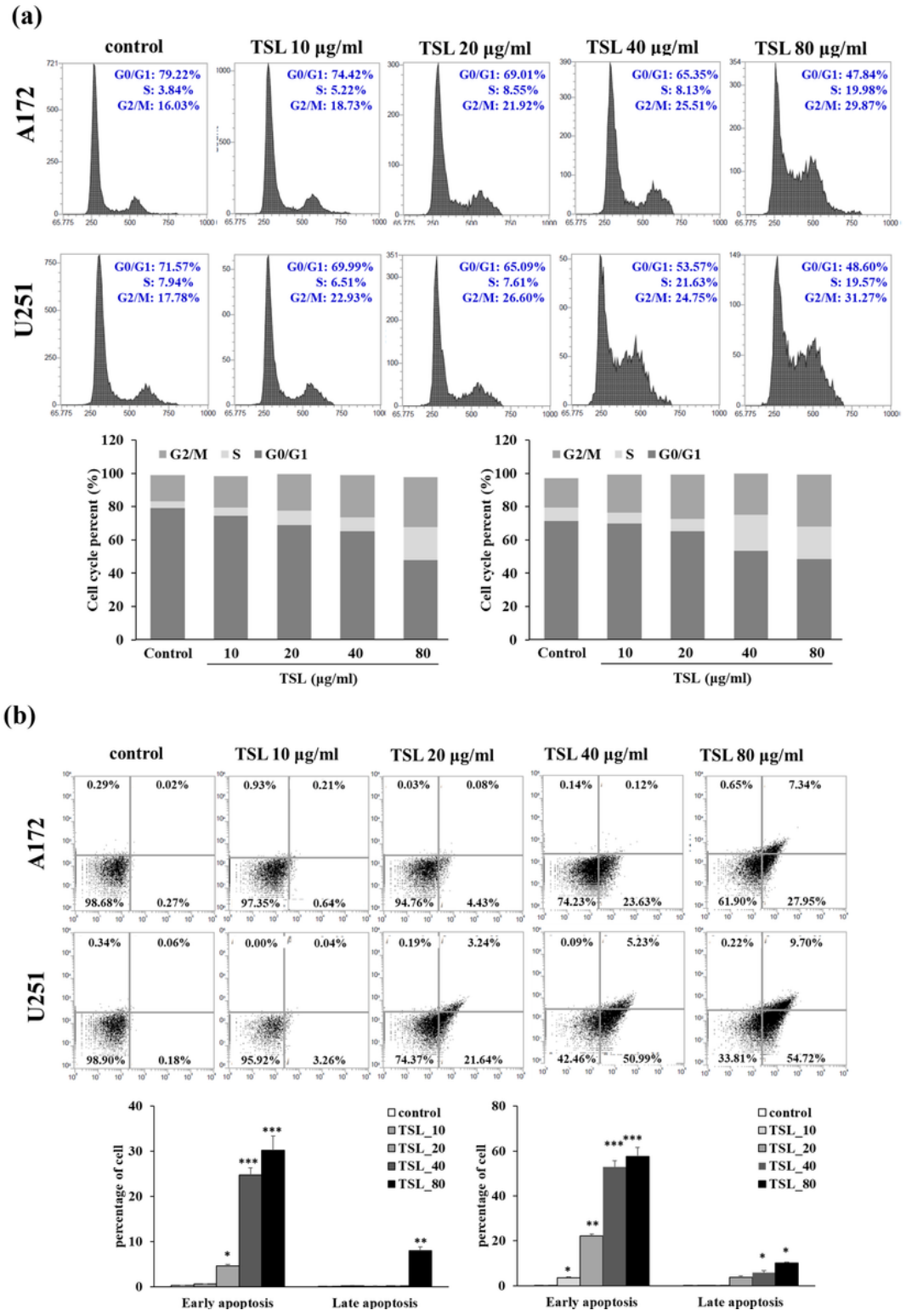

Figure 2

TSL induces apoptosis as well as cell cycle arrest in A172 and U251 GBM cells. (A) A172 and U251 cells were treated with different concentrations of TSL for 48 h, and then examined by flow cytometry to analyze the cell cycle. The proportion of cells in each cell cycle stage is shown in the graph. (B) The proportion of apoptotic cells was detected using Annexin V-FITC and propidium iodide staining. The lower panel shows percentages of cells in the early apoptosis (Annexin V+/PI-) together with late

apoptosis (Annexin V+/PI+) quarters were calculated as Annexin V positive cells for statistical analysis. All results are shown as mean ± s.d. from three independent experiments; ***p<0.001, **P < 0.01, *P < 0.05 compared with the indicated control.

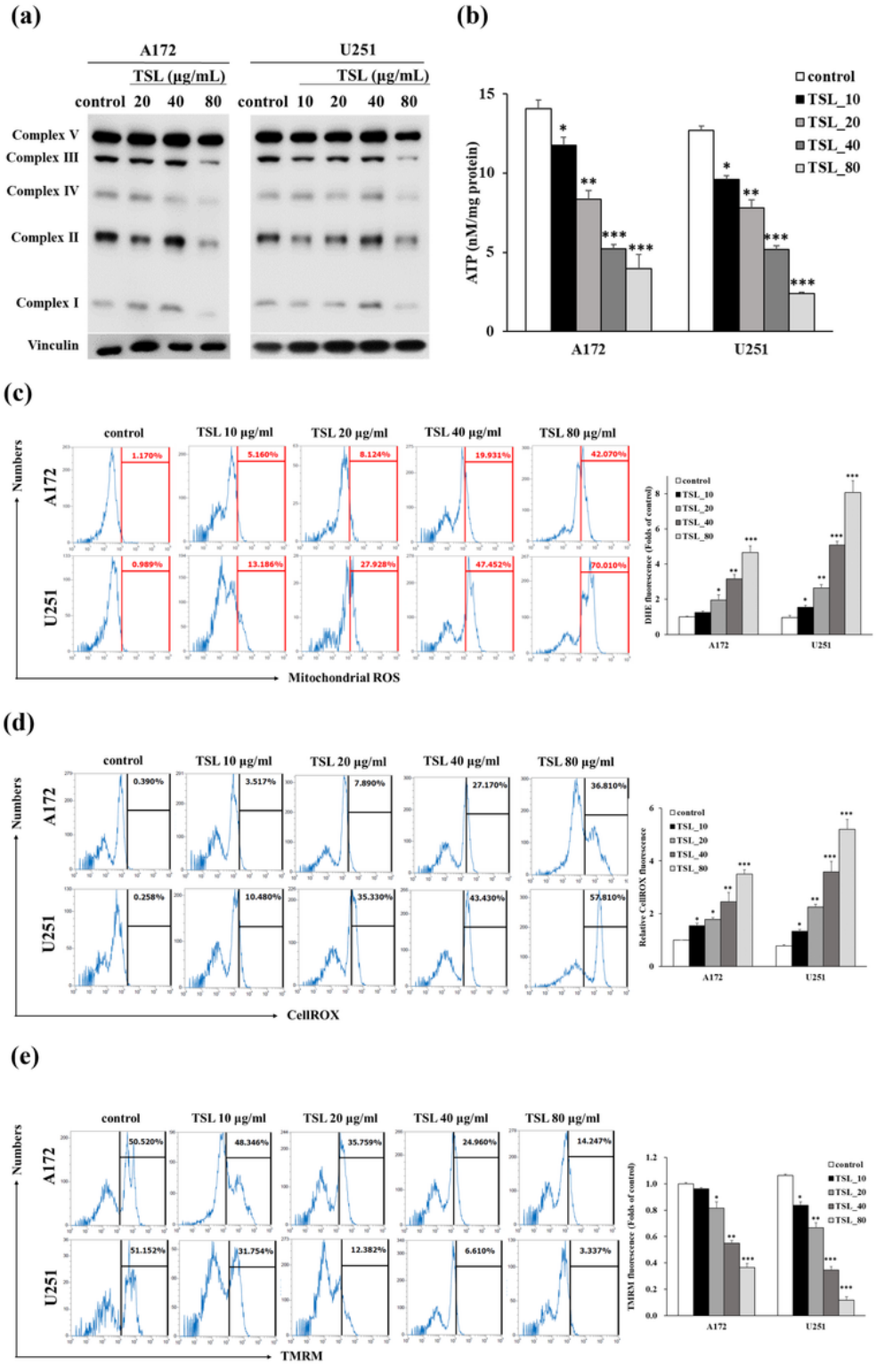

Figure 3

Increases in mitochondrial ROS associated with ΔΨm decreases in TSL-treated cells. (A) Effect of TSL on the expression of OX-PHOS-related protein complexes in A172 and U251. (B) Normalized ATP measurements in A172 and U251 cells. (C) mitochondria ROS, (D) cytosolic ROS and (E) ΔΨm levels were measured using flow cytometry and fluorescence microscopy with DHE Deep Red, CellROX Deep green, and TMRM Deep Red staining, respectively, and indicated by representative histograms are shown in parallel with bar graphs showing the relative TMRM mean relative fluorescence intensity. All results are shown as mean ± s.d. from three independent experiments; ***p<0.001, **P < 0.01, *P < 0.05 compared with the indicated control.

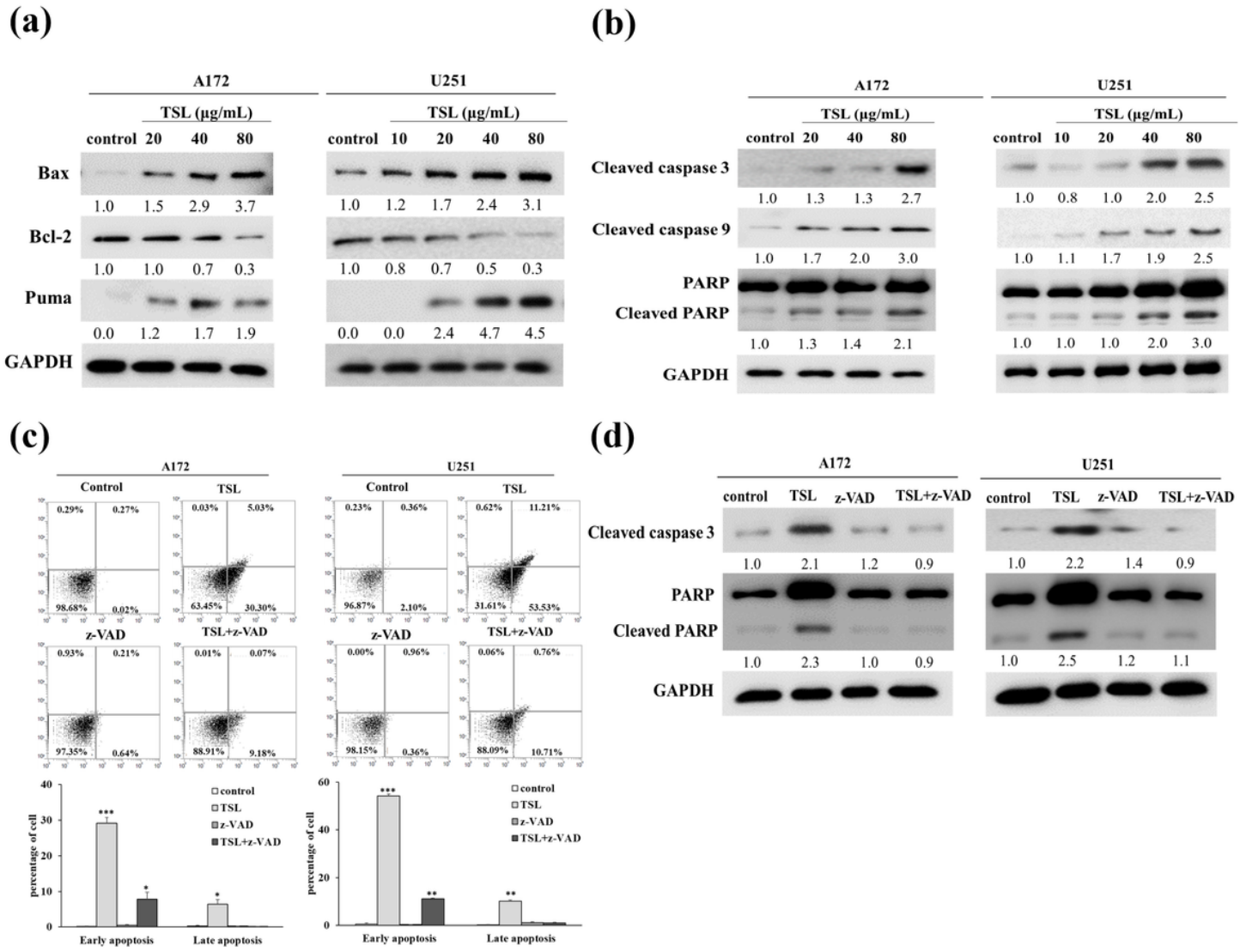

Figure 4

TSL induces apoptotic cell death via the intrinsic mitochondrial and caspase-dependent pathway. (A) Effect of TSL on the expression of PUMA, Bax and Bcl-2 proteins in GBM cell line. (B) Representative images of cleaved caspase 9, cleaved caspase 3, and PARP/cleaved PARP western blots. (C) The pan-caspase inhibitor z-VAD-FMK blocks caspase-dependent apoptosis induced by TSL in GBM. A172 and U251 cell lines were pretreated with or without the pan-caspase inhibitor z-VAD-FMK (20 μM) for 1 h and

then incubated with TSL (80 ug/mL) for 48 h. Then, apoptosis was measured using flow cytometry by Annexin V-FITC and PI staining. (D) Representative images of cleaved caspase 3, and PARP/cleaved PARP western blots. All results are shown as mean ± s.d. from three independent experiments; ***p<0.001, **P < 0.01, *P < 0.05 compared with the indicated control.

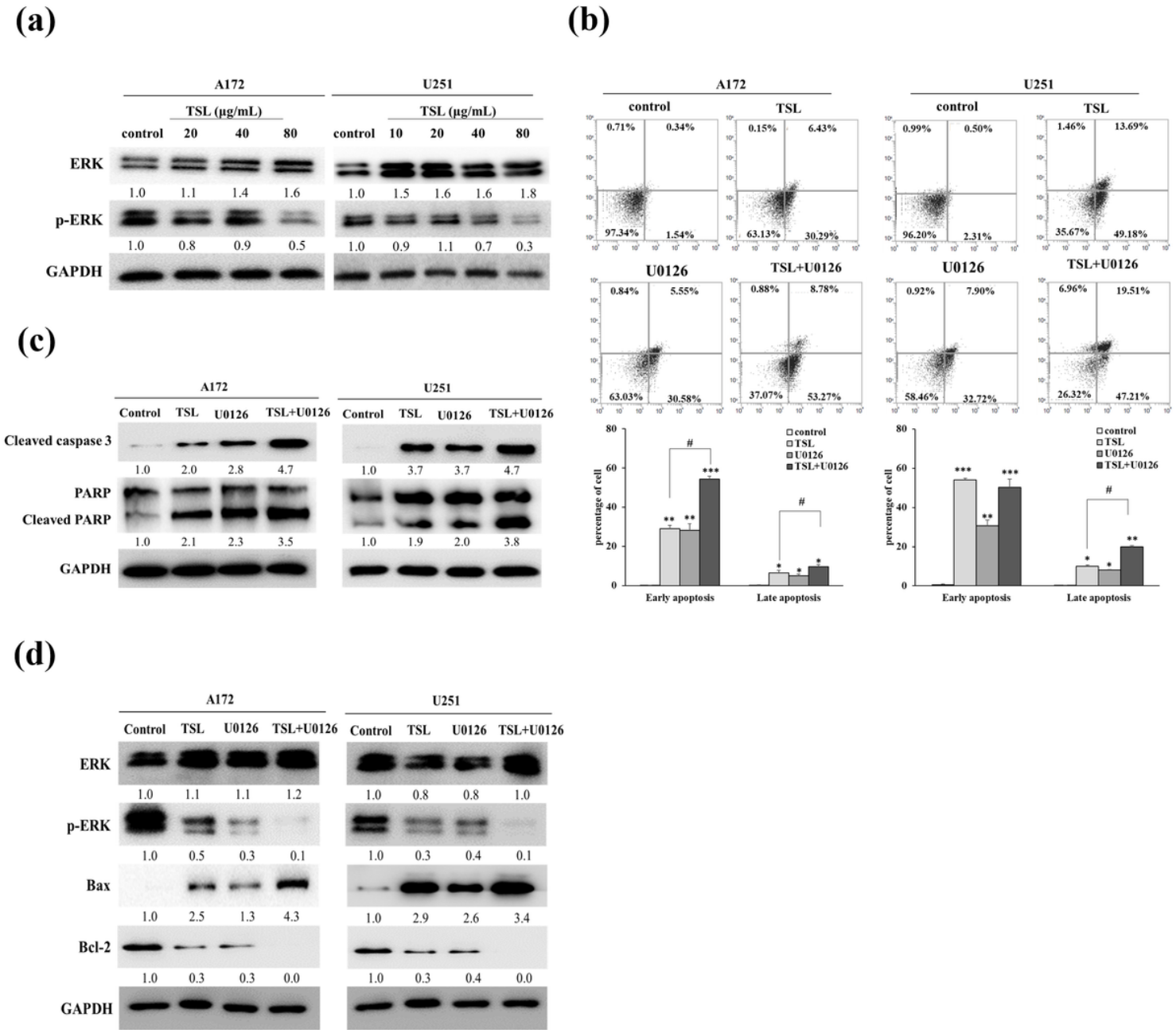

Figure 5

ERK activation is required for apoptosis induction by TSL treatment. (A) A172 and U251 cells were incubated with different concentrations of TSL for 48 h, cells were harvested and detected for ERK1/2 and p-ERK1/2 by western blot analysis. (B) The effects of MEK/ERK inhibition by U0126 on the cell death.

A172 and U251 cells were treated with TSL (80 ug/mL) in the absence or presence of U0126 (10 μM) for 48 h. The proportion of apoptotic cells was detected with Annexin V-FITC and propidium iodide staining. (C) Representative images of cleaved caspase 3, and PARP/cleaved PARP western blots. (D) Representative images of ERK1/2, p-ERK1/2, Bax and bcl-2 western blots. All results are shown as mean ± s.d. from three independent experiments; ***p<0.001, **P < 0.01, *P < 0.05 compared with the indicated control.

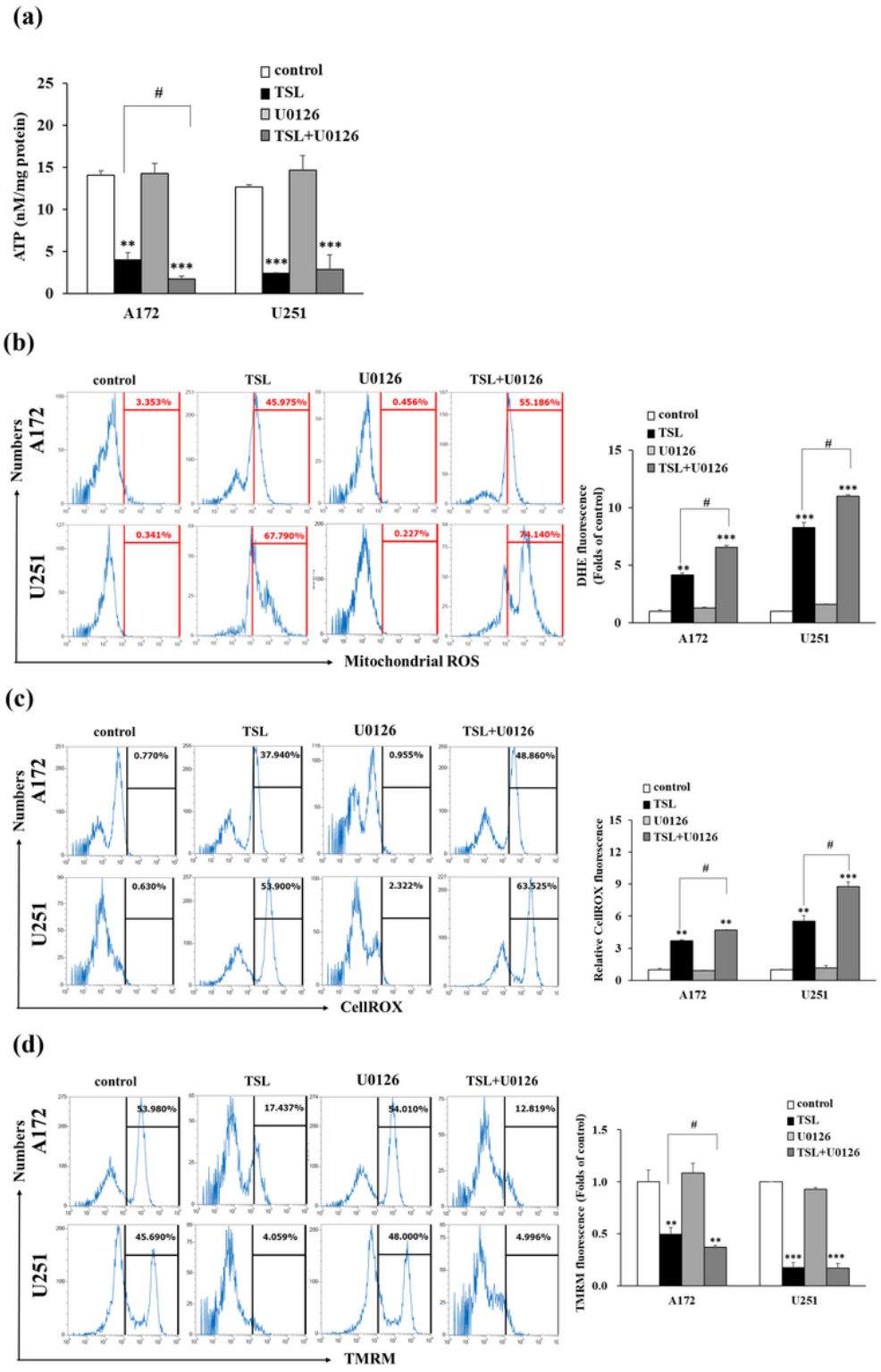

Figure 6

Effect of MAPK inhibitors on mitochondrial function in A172 and U251 cells subjected to TSL. (A) A172 and U251 cells were incubated with different concentrations of TSL for 48 h, cells were harvested and detected for normalized ATP measurements. (B) mitochondrial ROS, (C) cytosolic ROS and (D) ΔΨm levels were measured using flow cytometry and fluorescence microscopy with DHE Deep Red, CellROX Deep green, and TMRM Deep Red staining, respectively, and indicated by representative histograms are shown in parallel with bar graphs showing the relative TMRM mean relative fluorescence intensity. All results are shown as mean ± s.d. from three independent experiments; ***p<0.001, **P < 0.01, *P < 0.05 compared with the indicated control.

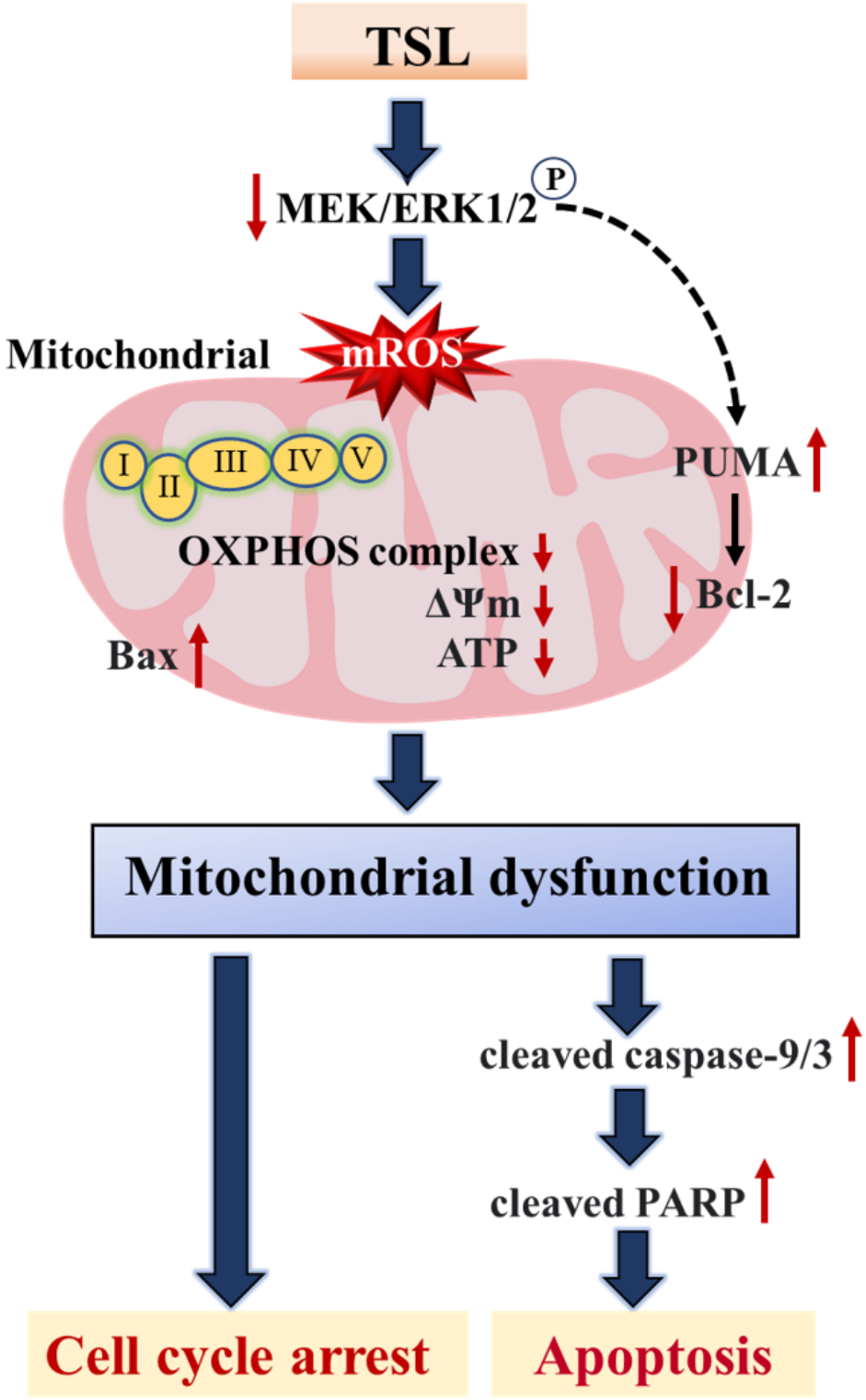

Figure 7

Model for TSL treatment in GBM cells. After TSL treatment, MEK/ERK pathway was inhibited which lead to mitochondria ROS degeneration, then decreased OXPHOS complexes that attenuated ATP production, and caused mitochondria dysfunction eventually. Upregulation of pro-apoptotic proteins (Bax and Puma) and downregulation of anti-proapoptotic protein (Bcl-2) were also illustrated and leaded to mitochondria

dysfunction. Finally, caspase-dependent apoptosis (cleaved caspase-3, 9 and PARP) was induced in the last event under TSL treatment in GBM cells.

Supplementary Files

This is a list of supplementary files associated with this preprint. Click to download.

- ImagesinFigureTSL.pdf